JET-IMPACT NEBULIZATION FOR SAMPLE INTRODUCTION IN
INDUCTIVELY COUPLED PL..(U) INDIANA UNIV AT BLOOMINGTON
DEPT OF CHEMISTRY   M P DOHERTY ET AL. 23 SEP 83
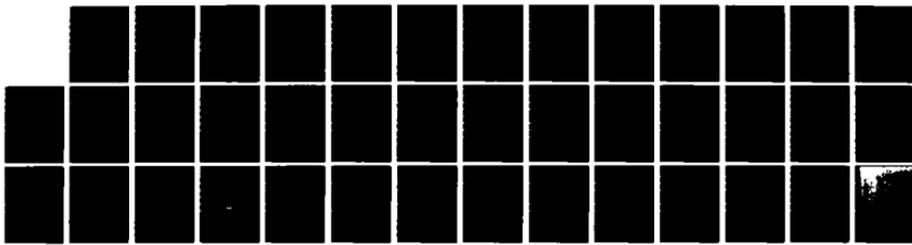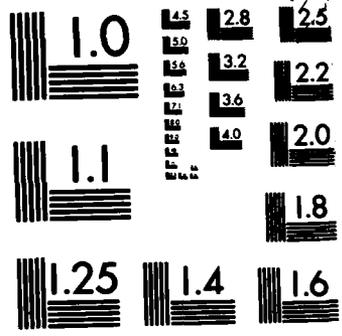
MICROCOPY RESOLUTION TEST CHART

NATIONAL BUREAU OF STANDARDS-1963-A

SECURITY CLASSIFICATION OF THIS PAGE *(When Data Entered)*

REPORT DOCUMENTATION PAGE		READ INSTRUCTIONS BEFORE COMPLETING FORM
1. REPORT NUMBER INDU/DC/GMH/TR-83-57	**2. GOVT ACCESSION NO.** AD-A133 152	**3. RECIPIENT'S CATALOG NUMBER**
4. TITLE *(and Subtitle)* Jet-Impact Nebulization for Sample Introduction in Inductively Coupled Plasma Spectrometry		**5. TYPE OF REPORT & PERIOD COVERED** Interim Technical Report
		6. PERFORMING ORG. REPORT NUMBER 66
7. AUTHOR(s) M. P. Doherty and G. M. Hieftje		**8. CONTRACT OR GRANT NUMBER(s)** N14-76-C-0838
9. PERFORMING ORGANIZATION NAME AND ADDRESS Department of Chemistry Indiana University Bloomington, IN 47405		**10. PROGRAM ELEMENT, PROJECT, TASK AREA & WORK UNIT NUMBERS** NR 051-622
11. CONTROLLING OFFICE NAME AND ADDRESS Office of Naval Research Washington, D.C.		**12. REPORT DATE** 23 September 1983
		13. NUMBER OF PAGES 32
14. MONITORING AGENCY NAME & ADDRESS*(if different from Controlling Office)*		**15. SECURITY CLASS. (of this report)** UNCLASSIFIED
		15a. DECLASSIFICATION/DOWNGRADING SCHEDULE

16. DISTRIBUTION STATEMENT *(of this Report)*

This document has been approved for public release and sale; its distribution is unlimited.

17. DISTRIBUTION STATEMENT *(of the abstract entered in Block 20, if different from Report)*

18. SUPPLEMENTARY NOTES

19. KEY WORDS *(Continue on reverse side if necessary and identify by block number)*

Sample introduction, nebulizer, inductively coupled plasma, atomic emission spectrometry

20. ABSTRACT *(Continue on reverse side if necessary and identify by block number)*

A novel, simple device for the production of liquid aerosol has been constructed and evaluated. In operation of this device, a sample solution is forced under pneumatic or mechanical pressure through an orifice of 25-60 micrometers in diameter. The resulting high-velocity stream of solution is directed onto a solid surface, thereby generating a fine aerosol. Details of nebulizer construction and operation are discussed and factors affecting nebulizer performance are examined. The utility of this nebulizer as a sample-introduction device for inductively coupled plasma spectrometry is explored.

(continued)

DD FORM 1473 EDITION OF 1 NOV 65 IS OBSOLETE UNCLASSIFIED

83 09 29 094

20. (continued)

When coupled with an ICP, the jet-impact nebulizer compares favorably with a conventional pneumatic nebulizer in terms of precision, linearity, detection limits, and efficiency. Moreover, aerosol production is independent of any gas flow, making the device potentially useful in low-gas-flow plasmas. However, clogging of the nebulizer orifice with particulate matter can be a problem unless solutions are pre-filtered.

OFFICE OF NAVAL RESEARCH

Contract N14-76-C-0838

Task No. NR 051-622

JET-IMPACT NEBULIZATION FOR SAMPLE INTRODUCTION

IN INDUCTIVELY COUPLED PLASMA SPECTROMETRY

by

M. P. Doherty and G. M. Hieftje

Prepared for Publication

in

APPLIED SPECTROSCOPY

Indiana University
Department of Chemistry
Bloomington, Indiana 47405

23 September 1983

INTRODUCTION

Improved sample introduction could significantly enhance the analytical capabilities of inductively coupled plasma emission spectrometry. Not surprisingly, a substantial number of interesting approaches have been proposed for sample introduction into the ICP. Solid sampling has been investigated through the use of direct insertion techniques,[1,2] injection of powders,[3,4] laser vaporization techniques,[5-7] spark excitation,[8] and slurries.[9] Electrothermal methods,[10-13] direct insertion of sample solutions,[1,2,14,15] volatile molecule generation techniques,[16,17] direct injection of molecular gases,[18,19] and the introduction into an ICP of GC effluents[20-22] have also been explored. However, the greatest emphasis has been on the development of nebulizers, because so many analytical samples can be dissolved to form aqueous solutions. Nebulization devices include concentric[23-26] and cross-flow[27-30] pneumatic systems, fritted discs,[31] and Babington nebulizers.[32-37] Ultrasonic devices have been extensively investigated as well,[3,38-40] and have provided greater sensitivity for certain samples.[41]

Because the sample channel of an ICP discharge cannot easily accomodate a large flow of gas, an acceptable nebulizer for ICP spectrometry must operate effectively on a modest supply of argon, ordinarily below 2 L/min. Ultrasonic nebulizers enjoy a particular advantage over pneumatic systems; they require gas only to transport the sample aerosol and not to produce it. Unfortunately, ultrasonic generators are often complex, costly, and less reliable than pneumatic nebulizers. Other methods which do not require a gas flow should be explored. One such method involves the disruption of a high-speed jet of sample solution at impact upon a solid surface. The goal of the present study is the design and evaluation of a nebulizer based on this principle for the introduction of analyte solutions into an ICP. This device is termed the jet-impact nebulizer (JIN).

1

The principles of operation of the JIN[42] were known long before ICP spectroscopy became a popular analytical method. However, the device has seen little use recently, chiefly because it requires that solutions be forced through a small orifice. Finer aerosols are produced more efficiently from jets formed in narrower orifices; unfortunately, smaller orifices are more susceptilbe to obstruction. One recent application of a kind of JIN has been as an interface between a liquid chromatograph and a direct-current plasma.[43] In this application, particulate matter in an analytical sample is excluded before the nebulization step, thereby minimizing the risk of orifice obstruction. Because the JIN produces aerosol without any nebulizing gas, it is particularly well suited for use with low-flow ICP systems[44,45] or in applications such as sample modulation.[46]

In the present embodiment of the JIN, sample solution is forced pneumatically or mechanically through an orifice of 20 to 100 micrometers in diameter, to form a narrow, high-velocity jet of liquid. If this jet is allowed to travel through space, it begins to oscillate on the axes perpendicular to the axis of travel. At some characteristic distance from the orifice, these oscillating instabilities lead to disruption of the jet into droplets, whose diameter is of the order of the diameter of the jet. If a solid impact surface is positioned in the path of the jet at the point where instabilities have become pronounced, the kinetic energy of the jet can contribute effectively to jet rupture. The oscillating instabilities of the jet are enhanced by the impact, and much finer droplets are thus produced.

The nebulizer constructed in this study proved to be suitable for use in atomic emission spectrometry and provided low drift, low detection limits, and extended linear calibration curves. Occasional instablities of unknown origin were unfortunately noted. Several variables affecting nebu-

lizer performance were studied, including the orifice size and shape, jet velocity, analyte solution viscosity and surface tension, aerosol transport system, distance traveled by the jet, and angle of incidence of the jet upon the impact surface.

I. EXPERIMENTAL

Aerosol Production and Transport

Two types of orifices employed in the production of liquid sample jets are shown in Fig. 1. The orifice depicted in Fig. 1a was constructed by fire-polishing 1 mm o.d. glass capillaries to inside diameters of 20 to 100 micrometers. For the other kind of orifice (Fig. 1b), precisely drilled jewels of synthetic ruby (corundum) were used. The particular jewels used in this study are Seitz friction-balance watch jewels, and were purchased at a cost of about one dollar each at a local jewelry supply company; orifice diameters of 60 to 140 μm are available in increments of 10 μm. Corundum pieces with orifice diameters as small as 25 μm are available (Seitz SA, American Laubscher Corporation, Farmingdale, Long Island, NY). Importantly, these jewels exhibit superb resistance to corrosion and wear, precise orifice geometry, and low cost. Each jewel is bonded by means of inert epoxy onto the base of a 22-gauge hypodermic needle from which the shaft has been removed. This latter kind of orifice was employed for most experiments reported here.

Sample solutions were contained in polyethylene beakers within brass or steel vessels under argon pressure, as shown in Fig. 2. Argon was selected as the pressurizing agent to minimize the effects of dissolved gas on plasma performance. Of course, other pressurized gases could be employed. The argon pressure, controlled with a single-stage regulator (Air Products, Inc. Allentown, PA) forces sample solutions up a teflon dip-tube and through a

small membrane filter (Catalogue #LCWP 01300, Millipore Corp., Bedford, MA). The filtered solution is transported through flanged teflon tubing assembled with standard 1/4-28 low-pressure liquid-chromatography fittings, couplings and adapters (Rainin Instrument Co., Woburn, MA). For flow-injection experiments, a six-port rotary injection valve with a 0.5 mL sample loop (Rainin) is incorporated between the pressure vessel and the nebulizer orifice.

The jet of sample solution is forced against a glass impact surface, fixed at a distance of between 1 and 5 cm from the orifice. Of the various impact surfaces and arrangements that were explored, the most satisfactory is shown in Fig. 3. The impact surface is a fire-polished glass plate, 20 mm x 6 mm x 3 mm, fixed at the end of a length of 5-mm glass rod. The rod is friction-fitted through a 5-mm hole in a polytetrafluoroethylene aerosol-chamber endpiece. A second hole in the endpiece, fitted with a ¼-28 thread, is used to connect the sample delivery tubing to a luer adapter, onto which the jewel fitting is secured. This endpiece design permits the experi-menter to locate the impact surface directly in the path of the liquid jet, and at any desired distance from the orifice. The entire assembly is sealed by means of an O-ring inside an aerosol chamber constructed of 35-mm glass tubing, similar in design to the chamber of Schutyser and Janssens.[47] The aerosol collection funnel is situated 10 cm from the mouth of the chamber to provide room for the glass impact surface. A carrier-gas en-trance port is located 4 cm from the mouth of the chamber.

The performance of the jet-impact nebulizer was compared with that of a concentric glass nebulizer constructed according to the procedure of Scott.[26] Sample solutions are delivered to this concentric nebulizer at a rate of 2.40 mL/min by a peristaltic pump (Gilson Medical Electronics, Middletown, WI). A nebulizing argon flow between 0.86 and 1.41 L/min is

4

controlled and monitored with a needle valve and rotameter (Matheson Gas Products, Joliet, IL). This same rotameter is used to monitor carrier-gas flows for the JIN. The concentric nebulizer is sealed with an O-ring at the mouth of a glass aerosol chamber equipped with a central aerosol-collection funnel.[47]

The exit ports of both aerosol chambers are connected by 12-cm lengths of 3/16" tygon tubing to a glass "Y" tube. The third arm of the "Y" is connected by an 8-cm length of tubing through an opening in the bottom of a copper radiation shield to the aerosol inlet port of the plasma torch.

PLASMA

Two different ICP torches were employed in the present study. Because the concentric glass nebulizer had already been used extensively with a standard 20-mm o.d. torch, this same torch was employed for experiments involving a direct comparison of the two nebulizers. The 20-mm torch operates on 15 L/min coolant argon, 0.42 L/min plasma argon, and 1.25 kW forward RF power. For many other experiments, a 14-mm o.d. miniature torch was employed.[45] This smaller torch operates on 9.8 L/min coolant argon with no plasma argon at 1.0 kW forward RF power. Plasmas are formed in both torches with radio-frequency power generated and controlled by a 2.5 kW, 27.12 MHz instrument (Plasma-Therm, Inc., Kresson, NJ). Gas flows are controlled with needle valves and rotameters.

OPTICS AND DETECTION

A 10-cm focal length, 5-cm diameter quartz lens images the plasma at unity magnification onto the entrance slit of a 0.35-meter Czerny-Turner f/7 scanning monochromator (Heath Co., Benton Harbor, MI). Entrance and exit slits were set at 50 μm wide and 10 mm high. Because the ICP is situated on

5

a translatable platform, any region of the discharge can be viewed by the
fixed optical system. Unless otherwise noted, light was gathered from a
region 20-30 mm above the load coil in the center of the sample channel. A
photomultiplier tube (1P28A, RCA, Lancaster, PA), located at the exit slit
of the monochromator, was biased at 800 volts. The photocurrent from the PMT
was converted to a proportional voltage by a current amplifer (Model 427,
Keithley Instruments, Inc., Cleveland, OH), with a risetime (90%) of 100
msec.

The output of the amplifier was monitored simultaneously by a digital
multimeter (Model 179, Keithley), a strip-chart recorder (Model SR-204,
Heath), and a laboratory minicomputer (MINC-11, Digital Equipment Corp.,
Maynard, MA). BASIC software was written to collect, manipulate, display,
and store experimental data. The various programs included assorted opera-
tor prompts; text displayed on a CRT directs operator input of sampling
time, element, concentration, nebulizer type, and other information to be
stored with each set of numerical data.

REAGENTS

Stock solutions were prepared as suggested by Dean and Rains[48] with
reagent-grade metals, salts, and acids. Analyte solutions were prepared by
suitable dilution.

PROCEDURES

Detection limits for the jet-impact nebulizer and the concentric glass
nebulizer were computed as the concentration of analyte required to produce
a signal equal to 2.12 times the standard deviation of five background
measurements.[49] Detection limits are based on the extrapolation of signal
levels from the average of 5 measurements of dilute solutions. For each
element, viewing height in the plasma and nebulizer gas flow were optimized

6

to produce greatest signal-to-background ratios; optimal values are listed in Table I. Analyte concentrations were selected to be between 1 and 2 orders of magnitude above the detection limit. Each signal and blank measurement was taken as the average of 500 data points collected over a period of 20 seconds. Signal and blank measurements were alternated, with a pause of at least five system time constants between measurements.

The standard deviation of each group of 500 computer-stored data points was calculated and combined with four similar sets to yield an average standard deviation. This figure, the average noise, is useful in assessing high-frequency fluctuations which might be caused by the nebulizer.

For the determination of drift, 500 signal-averaged measurements were collected over a period of two hours. Each of the 500 measurements was taken as the average of 500 data points collected over a period of 10 seconds. The relative standard deviation of the 500 averaged measurements was defined as the system drift. Drift was measured at the Ca II 393.4 nm line with 1 µg/mL Ca introduced by either the jet-impact or concentric nebulizer, or with the aerosol-free ICP operating on 1.08 L/min of dry carrier argon.

For flow-injection measurements, sample solution is drawn into a 0.5 mL sample loop by means of a syrings. Meanwhile, a constant stream of distilled, deionized water flows from the pressure vessel through the six-port injector valve to the nebulizer. When the valve is actuated, the slug of solution in the loop is injected into the stream of water. The first trace of the sample reaches the jet-impact nebulizer 10 seconds later, after traveling through a 60-cm length of teflon tubing. During this transit time, the operator must si_ al the computer to initiate data collection. Five hundred data points are then collected over a period of 60 seconds,

and displayed on a video terminal. The signal appears as a diffusionally broadened peak. Forty seconds after the first data set is completed, another set of 500 data points is collected. Because only distilled water is being nebulized during this latter period, the second data set serves as a blank measurement. These data, plotted with the peak, ordinarily appear as a flat baseline. The data from each set in a pair are summed and compared, and used by the computer to calculate the area between the signal and blank traces in units of microamp-seconds of photocurrent. This area, which is proportional to analyte mass, enables the computer to generate calibration curves. For each curve, five measurements are averaged for each analyte concentration.

A useful diagnostic for JIN performance is the nebulizer efficiency, which can be defined as the fraction of sample solution which leaves the impact surface in the form of droplets. Here, the nebulizer efficiency was calculated as $(1 - \frac{m_d}{m_s})$, where m_s is the quantity of solution fed to the nebulizer and m_d the amount drained as liquid from the impact surface. This fraction is commonly 0.25-0.30, in agreement with earlier workers who employed non-aqueous solutions.[43] Measurements of drainage from the impact of a jet producing no aerosol show that this figure is reliable to within 2% of the sample flowrate. Clearly, losses in the aerosol chamber and during sample transport will reduce substantially the overall aerosol delivery efficiency.[50] However, the nebulizer efficiency serves as a particularly quick and convenient way to assess whether nebulizer variables have been properly adjusted.

II. RESULTS AND DISCUSSION

NEBULIZER OPERATION

The performance of the new nebulizer is a function of several vari-
ables, critical among which is the geometry of the orifice used to produce
the jet. Early work was performed with glass capillaries (cf. Fig. 1a)
whose tips had been constricted by fire-polishing to produce orifices be-
tween 20-100 μm. Unfortunately, such orifices often were not quite circular
or produced liquid jets which would exit the capillary at unsuitable angles.
Additionally, the long funnel-shaped glass pathway toward the orifice en-
couraged the accumulation of particulate matter, which subsequently obstruc-
ted the liquid flow. Orifices of this type proved to be fragile and diffi-
cult to construct and maintain.

For these reasons, a second orifice type was investigated. This alter-
native orifice is a shallow circular hole in a jewel of corundum, epoxied
onto a luer fitting. The shallowness of the hole leads to fewer problems
with particulate accumulation or salt encrustation; solutions of 10% (by
weight) NaCl have been run repeatedly with no observed encrustation. The
shallow hole also exerts less drag on the analyte solution flowing through
it, permitting higher solution flowrates through orifices of a given dia-
meter (cf. Fig. 4). The precision of the corundum orifice size and shape is
sufficient that liquid jets formed with three different 60-μm jewels were
found to behave nearly identically. These devices are extremely durable;
none of the jewels used throughout these experiments has failed. Jewels
which became partially clogged were easily cleaned with brief backflushing.

Jewels with holes from 60 to 140 μm were examined and provided solution
uptake rates of 4-28 mL/min at regulator-accessible operating pressures.

High uptake rates make the larger jewels undesirable for use in spectrochem-
ical analysis. Additionally, the increase in droplet size with the larger
jewels is sufficient to be easily observed with the unaided eye. For these
reasons, the 60-µm jewel was selected for further experiments, in spite of
its somewhat greater susceptibility to obstruction.

Several methods have been explored for pumping solutions to the JIN,
each with its own advantages and disadvantages. An inexpensive pressurized
vessel (cf. Fig. 2), used in most of these experiments, provides an extreme-
ly constant flow of solution. However, changing sample solutions is incon-
venient and time-consuming, making flow-injection techniques more attrac-
tive. A syringe pump also provides a reasonably steady flow, but is equally
cumbersome and is limited to modest solution volumes. Peristaltic and
liquid-chromatography (LC) pumps are more convenient to operate. However,
pulsations generated by a peristaltic pump have been found to be disadvanta-
geous for the JIN and a pulse-free LC pump would significantly increase the
cost and complexity of the nebulizer. For routine use, therefore, flow-
injection methods are suggested and were adopted.

The distance traveled by the jet prior to impact proves to be a crit-
ical variable. If the impact surface is placed very near the orifice, no
aerosol is produced, presumably because the natural instability of the jet
has not developed sufficiently at such a short distance. Under these circum-
stances, the drainage from the impact surface is equal to the flowrate
through the jewel, and the nebulizer efficiency is zero. If the impact
surface is slowly moved away from the orifice, a critical distance is reach-
ed, at which the nebulizer efficiency abruptly rises to over 0.25. Inter-
estingly, at this same distance from the orifice one can first visually
observe a periodic instability in the jet. This critical distance depends
on the physical properties of the solution, the velocity of the jet, and the

10

orifice diameter. In general, the critical distance increases with increas-

ing jewel size and jet velocity, as illustrated in Fig. 5. Several excep-

tions to this trend were noted; some jewels above 100 μm did not perform as

expected, and slightly oval-shaped glass capillaries or partially obstructed

jewels exhibited critical distances well below predicted values, caused

presumably by instability introduced at the source of the jet.

Figure 6 shows the effect the jet travel distance has on a copper

emission signal at the 324.7-nm atom line. At impact distances below the

critical distance, the signal does not exceed the background level. The

critical distance is marked by the steeply rising portion of the plot at

19mm. Noise on the signal near this point is substantial; modest changes in

flow rate, surface drainage, etc. can cause aerosol production to fluctuate

dramatically. Well beyond the critical distance, the signal decreases;

deceleration of the jet reduces its kinetic energy and leads to less effec-

tive jet rupture. Signal-to-noise ratios appear greatest at distances 1.5-2

times the critical distance. These trends are independent of flow rate or

orifice size.

Significantly, the critical distance shown in Fig. 6 for the 60-μm

orifice nebulizer operated at 60 psig differs from the value shown in Fig.

5. This difference is believed to be caused by an acoustic resonance in the

aerosol chamber used to obtain the data in Fig. 6; in contrast, observations

recorded in Fig. 5 were for the same nebulizer operated outside the chamber.

This hypothesis is supported by the observation that a 60-μm orifice located

19-25 mm from the impact surface is incapable of producing a noticeable

spray. However, if a 35-mm chamber or a small beaker or flask is positioned

around the impact surface, aerosol production is initiated.

In the JIN, the critical distance for nebulization varies with the average forward velocity of the jet, which is calculated as the quotient of the flow rate divided by the orifice area, and which is controlled by the argon pressure over the sample solution. The optimal jet velocity was determined on the basis of sample utilization efficiency, defined as the ratio of ICP emission signal to uptake rate for a 10 mg/L Cu solution. For jet velocities between 21-39 m/sec and with the impact surface optimally situated for each velocity, sample utilization efficiency varies as shown in Fig. 7. At low jet velocities, limited kinetic energy in the jet leads to poor nebulization. At higher velocities, flooding of the impact surface with excess solution hinders nebulization. In the range between 28 and 33 m/sec, corresponding to driving pressures of 70-90 psig with a 60-μm orifice, the nebulizer most efficiently converts analyte solution to spectroscopically useful droplets. For later studies, 80 psig of argon was used to drive the fluid jet.

Aerosol delivery efficiencies of both the concentric and jet-impact nebulizers were measured from the increase in mass of a drying tube situated at the tip of the sample-injection tube of the ICP torch.[35] The mass of water collected over a period of several minutes was compared with the total solution flow into each nebulizer. This method for the estimation of efficiency is suitable for comparison of the two nebulizers used in this work; however, more elaborate procedures are recommended for a comparison with efficiencies measured in other laboratories.[51] The concentric nebulizer, operating on 1.03 L/min argon and 2.40 mL/min solution, demonstrated an efficiency of 0.8%, whereas the JIN, operating on 0.64 L/min carrier argon and 5.25 mL/min solution, yielded an efficiency of 0.5%. The low carrier gas flow rate for the JIN was chosen for two reasons. As Fig. 8 illustrates, the signal-to-background ratio is greatest for the JIN with a carrier gas

12

flow rate of about 0.6 L/min in a conventional (20 mm o.d.) ICP torch. Moreover, at greater carrier gas flows, condensation of the aerosol on transfer and torch tubes became problematic.

Aerosol delivery efficiency was measured also for a jet-impact nebulizer constructed from a glass-capillary jet (cf. Fig. 1a) situated 17 mm from a flat glass impact surface. The orifice in the capillary was slightly oval, and was measured with a calibrated microscope to be 41 and 44 μm across its narrowest and broadest axes respectively. Operated at 128 psig, this nebulizer demonstrated a solution uptake rate of 1.7 mL/min, and an efficiency of 2.5%. This evidence suggests that droplets small enough to be spectroscopically useful are much more efficiently produced through the shattering of a finer jet of solution.

Understandably, performance of the JIN depends upon the angle between the jet and the impact surface; best performance is obtained with impact at or near 90°. There appears to be little variation in performance for angles within 10° of normal. However, the nebulization efficiency decreases by 50% for an angle of 60° and by 83% for an angle of 30° to the impact surface. At angles below 25°, nebulization visibly ceases.

Nebulizer performance depends also on the location of impact on the glass surface. The shattering jet clears a small circular area ($\sim$ 1 mm in diam.) on the impact surface, around which a ring of excess solution accumulates and drains. If this circular area overlaps an edge of the glass, the nebulizer operation is dramatically altered. The nebulization efficiency increases substantially, often to over 0.50. However, the droplets that are formed are visibly much larger and produce analytical signals that are significantly lower and noisier. Not surprisingly, aerosol formed by impact on a surface edge can leave the surface with a high velocity perpendicular

to the edge. In fact, such an aerosol can be directed up a torch sample-injection tube even in the absence of carrier gas-flow. Unfortunately, this approach yields extremely noisy signals, rendering it unsuitable for quantitative work.

The drainage of excess solution away from the point of impact is significant in the formation of aerosol. The amount of aerosol which is produced fluctuates as the ring of accumulated solution expands and contracts with the formation and drainage of drops on the impact surface. Several methods of reducing these drainage fluctuations were investigated. Nebulization of a vertical jet on a horizontal surface was explored, as was nebulization on a non-wetting teflon surface. In another approach, small hydrophilic threads were situated near the point of impact to serve as wicks for drainage. Impact on fabric and fine metal and nylon screen was also investigated. None of these approaches led to increased signals or reduced noise. However, it has been observed that impact near the upper edge of a surface often yields steadier signals. Perhaps this approach reduces waste accumulation above the point of impact and thereby minimizes the effect of solution draining back to the point of impact.

Physical properties of the sample solution affect nebulizer performance. Various mixtures of glycerol and water, up to 60% glycerol by weight, were pumped through the nebulizer. As the relative viscosity increased, the flowrate through the jewel and the average jet veolcity decreased, thereby reducing the nebulization efficiency (cf. Fig. 7). This decrease in nebulization efficiency was due entirely to the lower velocity; when the pressure was adjusted to re-establish a jet velocity of 30 m/sec, the efficiency for all mixtures fell within the range of 0.25-0.28. Heavier glycerol mixtures had only slightly higher efficiencies, possibly as a consequence of their slightly lower surface tensions. For analytical use of

14

the nebulizer with highly viscous samples, a blank solution of matched viscosity would be recommended.

ANALYTICAL UTILITY OF THE JIN

The practical utility of the JIN as a sample introduction device for ICP spectrometry can be demonstrated through the measurement of limits of detection, S/N ratios, drift, and calibration curves. Because each component of an ICP spectrometer affects detection limits, a comparison of results from different spectrometers can be ambiguous. Therefore, detection limits were determined for both the glass-concentric and jet-impact nebulizers on the same system and under the same operating conditions. Through the use of the "Y"-tube described earlier, it was possible to perform back-to-back detection-limit measurements with the two nebulizer types simply by switching a valve directing the carrier argon to either of the devices.

Detection limits for six elements, listed in Table II, reveal that the JIN compares favorably with the concentric-glass nebulizer. Interestingly, for most elements the JIN signal level was 5-10 times as great as that from the concentric nebulizer, probably because of the higher solution uptake rate and the substantially longer residence time for the analyte introduced at lower carrier gas flowrates with the JIN. However, the background emission and hence the background noise were significantly higher with the lower JIN carrier-gas flow in the central channel of the ICP; as a result, detection limits for the two nebulizers were comparable.

Noise recorded during detection-limit measurements with both nebulizers has been used to calculate the signal-to-noise ratios listed in Table II. For these measurements, data were sampled at 25 Hz. In the studied frequency range, the JIN generally provides S/N ratios equal to or greater than those obtained with the concentric nebulizer.

15

Drift was measured as the RSD over a two-hour period for both nebu-
lizers, and for the ICP operating with 1.08 L/min of dry carrier argon. The
dry ICP demonstrated an RSD of 2.1%. Essentially linear upward drift was
observed at 393.4 nm. When operated with the concentric nebulizer, the ICP
demonstrated an RSD of 2.7%, including a rather uneven downward drift.
Modest signal shifts of 1-2 minutes duration were occasionally noted. When
operated with the JIN, the ICP signal had an RSD of 2.3%, including a brief
period of downward drift followed by a period of extremely steady signal.

A key advantage of ICP systems is their ability to provide calibration
curves which are linear over several orders of magnitude. An ICP with
sample introduction by jet-impact nebulization demonstrates this same advan-
tage. Figure 9 shows calibration curves for Ca II (393.4 nm) and Cu I
(324.7 nm) obtained with the flow-injection (FIA) technique described ear-
lier. Solutions of over 10,000 µg/mL of each element were easily introduced
into the ICP, but had to be measured at lower PMT bias voltages. Under the
operating conditions ordinarily used with the ICP, such high concentrations
saturate the PMT. At the lower end of the accessible concentration range,
the simple FIA procedure employed here sacrifices sensitivity; concentra-
tions of 10 ng/mL Cu and 1 ng/mL Ca could not be measured reliably. In
spite of these limitations, the calibrations curves are linear over four
orders of magnitude for both elements, with slopes of approximately one.
These data suggest that the nebulizer is suitable for use with FIA techni-
ques, which could clearly be exploited to greater advantage.[52]

III. CONCLUSIONS

The jet-impact nebulizer has proven to be suitable for use as a sample-
introduction device for ICP spectrometry. Performance of the nebulizer is

chiefly a function of the orifice size and shape, the distance traveled by the jet, and the jet velocity. Droplet production also varies with changes in the design of chambers and impact surfaces, the angle of incidence between the jet and impact surface, and the viscosity and surface tension of analyte solutions. A jet-impact nebulizer has been designed which is durable and inexpensive, and which provides reasonably low drift, low detection limits, and extensive linear calibration curves. However, sporadic problems with noise can prove troublesome. If partial obstruction of nebulizer orifices can be prevented, further work should focus on the use of smaller jewels, which would provide higher efficiencies and lower uptake rates. Unfortunately, sample introduction with the JIN can be cumbersome because the solution flowrate must be extremely steady and solutions must be completely free of particulate matter. The former requirement suggests the use of FIA techniques, which have proven to be convenient and effective with the nebulizer. Both requirements suggest the use of the device as an LC-ICP interface.[43] The production of droplets with the nebulizer is independent of gas flow, suggesting its use with miniaturized or low-flow ICP systems.

17

REFERENCES

1. E. D. Salin and G. Horlick, Anal. Chem. **51**, 2284 (1979).

2. D. Sommer and K. Ohls, Fresenius' Z. Anal. Chem. **304**, 97 (1980).

3. H. C. Hoare and R. A. Mostyn, Anal. Chem. **39**, 1153 (1967).

4. R. M. Dagnall, D. J. Smith, T. S. West, and S. Greenfield, Anal. Chim. Acta **54**, 397 (1971).

5. M. Thompson, J. E. Goulter, and F. Sieper, Analyst **106**,32 (1981).

6. K. Laqua, "Analytical Spectroscopy Using Laser Atomizers", in _Analytical Laser Spectroscopy_, N. Omenetto, ed., Chemical Analysis vol. 50, (Wiley-Interscience, New York, 1979), p. 85.

7. J. W. Carr, _Laser Vaporization of Solid Samples into ICP_ (M. Sc. thesis, University of Alberta, 1980).

8. H. G. C. Human, R. H. Scott, A. R. Oakes, and C. D. West, Analyst **101**, 265 (1976).

9. C. W. Fuller, R. C. Hutton, and B. Preston, Analyst **106**, 913 (1981).

10. D. E. Nixon, V. A. Fassel, and R. N. Knisely, Anal. Chem. **46**, 210 (1974).

11. A. M. Gunn, D. L. Millard, and G. F. Kirkbright, Analyst **103**, 1066 (1978).

12. M. J. Cope, G. F. Kirkbright, and P. M. Burr, Analyst **107**, 611 (1982).

13. K. Ohls and D. Sommer, Fresenius' Z. Anal. Chem. **296**, 241 (1979).

14. G. F. Kirkbright and Zhang Xing-Li, Analyst **107**, 617 (1982).

15. G. F. Kirkbright and S. J. Walton, Analyst **107**, 276 (1982).

16. K. A. Wolnik, F. L. Fricke, M. H. Hahn, and J. A. Caruso, Anal. Chem. **53**, 1030 (1981).

17. M. S. Black and R. F. Browner, Anal. Chem. **53**, 249 (1981).

18. S. J. Northway and R. C. Fry, Appl. Spectrosc. **34**, 332 (1980).

19. S. J. Northway and R. C. Fry, Appl. Spectrosc. **34**, 338 (1980).

20. D. L. Windsor and M. B. Denton, Anal. Chem. **51**, 1116 (1979).

21. D. L. Windsor and M. B. Denton, J. Chromatogr. Sci. **17**, 492 (1979).

22. M. A. Eckhoff, J. P. McCarthy, and J. A. Caruso, Anal. Chem. **54**, 165 (1982).

23. C. Veillon and M. Margoshes, Spectrochim. Acta **23B**, 503 (1968).

24. J. E. Meinhard, ICP Inf. Newsl. **2**, 163 (1976).

25. B. Bogdain, ICP Inf. Newsl. **3**, 491 (1978).

26. R. H. Scott, ICP Inf. Newsl. **3**, 425 (1978).

27. R. N. Knisely, H. Amenson, C. C. Butler, and V. A. Fassel, Appl. Spectrosc. **28**, 285 (1974).

28. D. L. Donahue and J. A. Carter, Anal. Chem. **50**, 686 (1978).

29. J. W. Novak, Jr., D. E. Lillie, A. W. Boorn, and R. F. Browner, Anal. Chem. **52**, 576 (1980).

30. B. Meddings, H. Kaiser, and H. Anderson, paper presented at International Winter Conference, Developments in Atomic Plasma Spectrochemical Analysis, San Juan, Jan. 1980.

31. C. T. Apel, T. M. Bieniewski, L. E. Cox, and D. W. Steinhaus, ICP Inf. Newsl. **3**, 1 (1977).

32. R. F. Suddendorf and K. W. Boyer, Anal. Chem. **50**, 1769 (1978).

33. J. F. Wolcott and C. Butler Sobel, Appl. Spectrosc. **32**, 591 (1978).

34. J. R. Garbarino and H. E. Taylor, Appl. Spectrosc. **34**, 584 (1980).

35. P.A.M. Ripson and L. de Galan, Spectrochim. Acta **36B**, 71 (1981).

36. B. Thelin, Analyst **106**, 54 (1981).

37. D. R. Heine, M. B. Denton, and T. D. Schlabach, Anal. Chem. **54**, 81 (1982).

38. R. H. Wendt and V. A. Fassel, Anal. Chem. **37**, 920 (1965).

39. P.W.J.M. Boumans and F. J. DeBoer, Spectrochim. Acta 27B, 391 (1972).

40. K. W. Olsen, W. J. Haas, Jr., and V. A. Fassel, Anal. Chem. 49, 632 (1977).

41. C. E. Taylor and T. L. Floyd, Appl. Spectrosc. 35, 408 (1981).

42. R. Herrmann, "Nebulizers and Burners", Flame Emission and Atomic Absorption Spectrometry, vol. 2: Components and Techniques, J. A. Dean and T. C. Rains, Eds. (Marcel Dekker, Inc., NY, 1971), p. 67.

43. P. C. Uden, B. D. Quimby, R. M. Barnes, and W. G. Elliot, Anal. Chim. Acta 101, 99 (1978).

44. G. R. Kornblum, W. van der Waa, and L. de Galan, Anal. Chem. 51, 2378 (1979).

45. R. N. Savage and G. M. Hieftje, Anal. Chem. 51, 408 (1979).

46. A. W. Steele and G. M. Hieftje, paper #51 at 8th annual FACSS meeting, Philadelphia, PA (1981).

47. P. Schutyser and E. Janssens, Spectrochim. Acta 34B, 443 (1979).

48. J. A. Dean and T. C. Rains, Flame Emission and Atomic Absorption Spectrometry, vol. 2: Components and Techniques (Marcel Dekker, Inc., NY, 1971), p. 322.

49. P. A. St. John, W. J. McCarthy, and J. D. Winefordner, Anal. Chem. 39, 1495 (1967).

50. R. F. Browner and D. D. Smith, Anal. Chem. 54, 1411 (1982).

51. D. D. Smith and R. F. Browner, Anal. Chem. 54, 533 (1982).

52. A. O. Jacintho, E. A. G. Zagatto, H. Bergamin F°, F. J. Krug, B. F. Reis, R. E. Bruns, and B. R. Kowalski, Anal. Chim. Acta 130, 243 (1981).

Table I.   Experimental conditions for detection-limit measurements with both concentric-glass and jet-impact nebulizers. Nebulizer argon flow for the JIN was 0.64 L/min in all cases. Nebulizer argon flow for the concentric nebulizer was varied as shown.

Element	Spectral line (nm)	ICP Viewing range (mm above load coil)	Concentric Nebulizer argon flow (L/min)
Ba	455.4	20-30	1.05
Ca	393.4	20-30	1.05
Cu	324.7	20-30	1.05
Fe	238.2	8-18	1.30
Mg	279.5	12-22	1.05
Zn	213.9	12-22	0.89

Table II. Comparison of Jet-impact (JIN) and concentric-glass nebulizers.

Element	Spectral line (nm)	Detection limits (ng/mL)		Signal-to-noise ratio		Concentration* (µg/mL)
		JIN	Concentric nebulizer	JIN	Concentric nebulizer	
Ba	455.4	5	5	20	6	0.1
Ca	393.4	1.4	0.7	3	6	0.01
Cu	324.7	6	7	5	5	0.1
Fe	238.2	24	60	88	12	1.0
Mg	279.5	1.1	1.5	53	20	0.1
Zn	213.9	9	14	76	10	1.0

*Concentration at which signal-to-noise ratio was measured.

FIGURE CAPTIONS

Figure 1.   Orifice types. (a) cross-sectional sketch of fire-polished
               glass capillary; actual o.d. 1 mm. (b) luer fitting with
               jewel orifice. (c) expanded cross-sectional sketch of jewel
               orifice; actual o.d. 1.0 mm.

Figure 2.   Diagram of nebulizer system. Details in text.

Figure 3.   Glass impact surface, nebulizer chamber endpiece, adapters
               and jewel fitting.

Figure 4.   Sample solution flow rate vs. orifice diameter at 80 psig
               applied pressure for both orifice types (cf. Figure 1). ⊙
               glass capillaries. * corundum jewels. Flowrates through
               jewels are more predictable and reproducible.

Figure 5.   The jet must travel a critical distance or it will not be
               effectively ruptured. This critical distance is greater when
               the jet velocity is greater or when a larger jet of solution
               is nebulized. ⊙ 60 psig. * 80 psig.

Figure 6.   Signal in ICP at copper 327.4 nm line for a 60-μm jewel
               nebulizer operating at 60 psig. Copper solution concen-
               tration - 10 mg/L.

Figure 7.   Sample utilization efficiency (ICP emission signal/ solution
               uptake rate) is a strong function of liquid jet velocity in

the JIN. A jet velocity of 30 m/sec corresponds to a
solution uptake rate of 5 mL/min.

Figure 8.   Optimal carrier gas flow rate for the JIN is about 0.6 L/min
              when used with a 20-mm o.d. ICP torch. Data represent
              measurements of 1.0 mg/L Zn at the 213.8 nm line.

Figure 9.   Calibration curves.
   △ Ca II (393.4 nm).
   ⊙ Cu I (324.7 nm).

(a)

(b)

(c)

Fig. 1

Fig. 1

Aerosol

Teflon
Tubing

Jewel
Orifice

Sample
Jet

Glass
Wall

Filter

Luer
Fitting

Sample
Solution

50-80
PSIG

Pressure
Vessel

Aerosol

Jewel

Jet

Glass
impact
surface

Luer fitting

"O"-ring

¼-28 L.C.
fitting

Nebulizer
chamber
endpiece

Teflon
tubing

Fig. 3

FLOWRATE (ml/min)

ORIFICE DIAMETER (μm)

Fig.

FIG. 5

CRITICAL DISTANCE (mm)

JEWEL DIAMETER (μm)

DISTANCE TO IMPACT (mm)

Cu SIGNAL (relative)

Fig 6

SIGNAL/UPTAKE
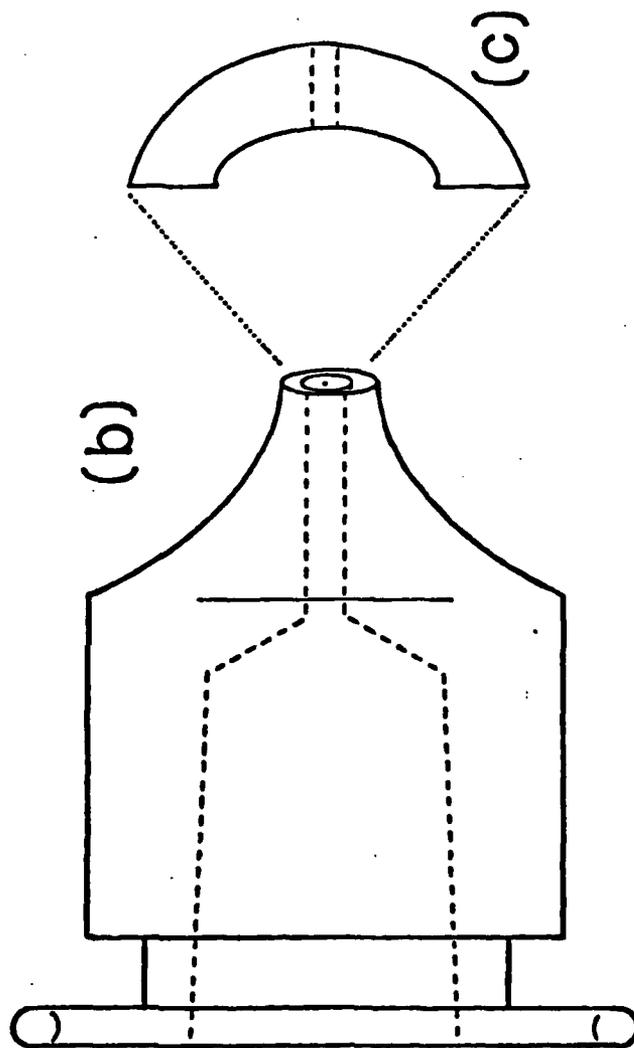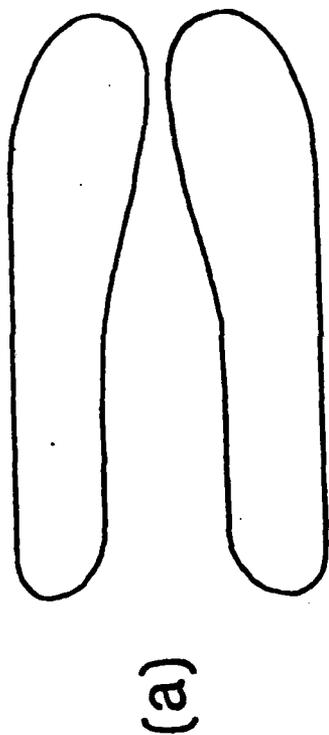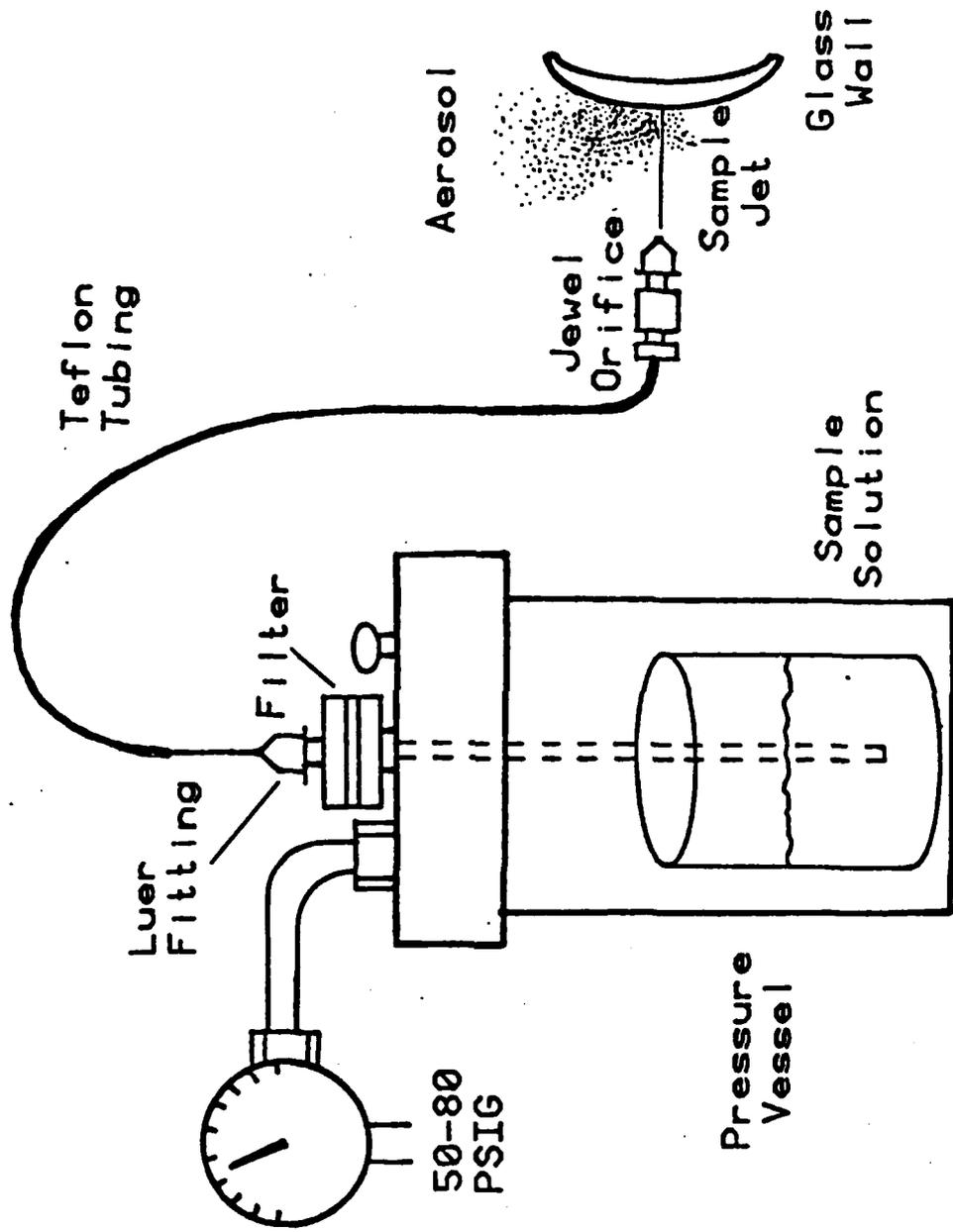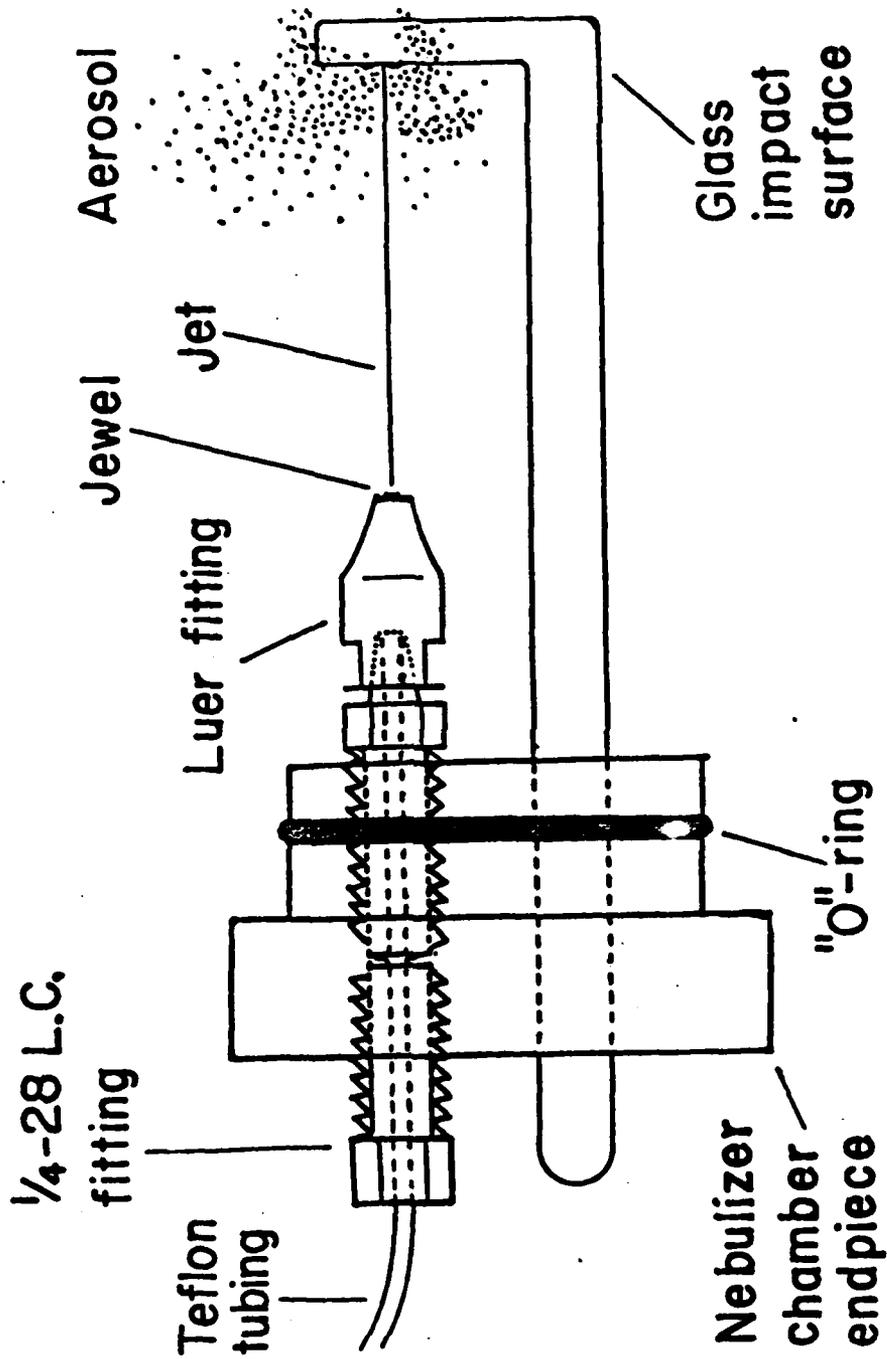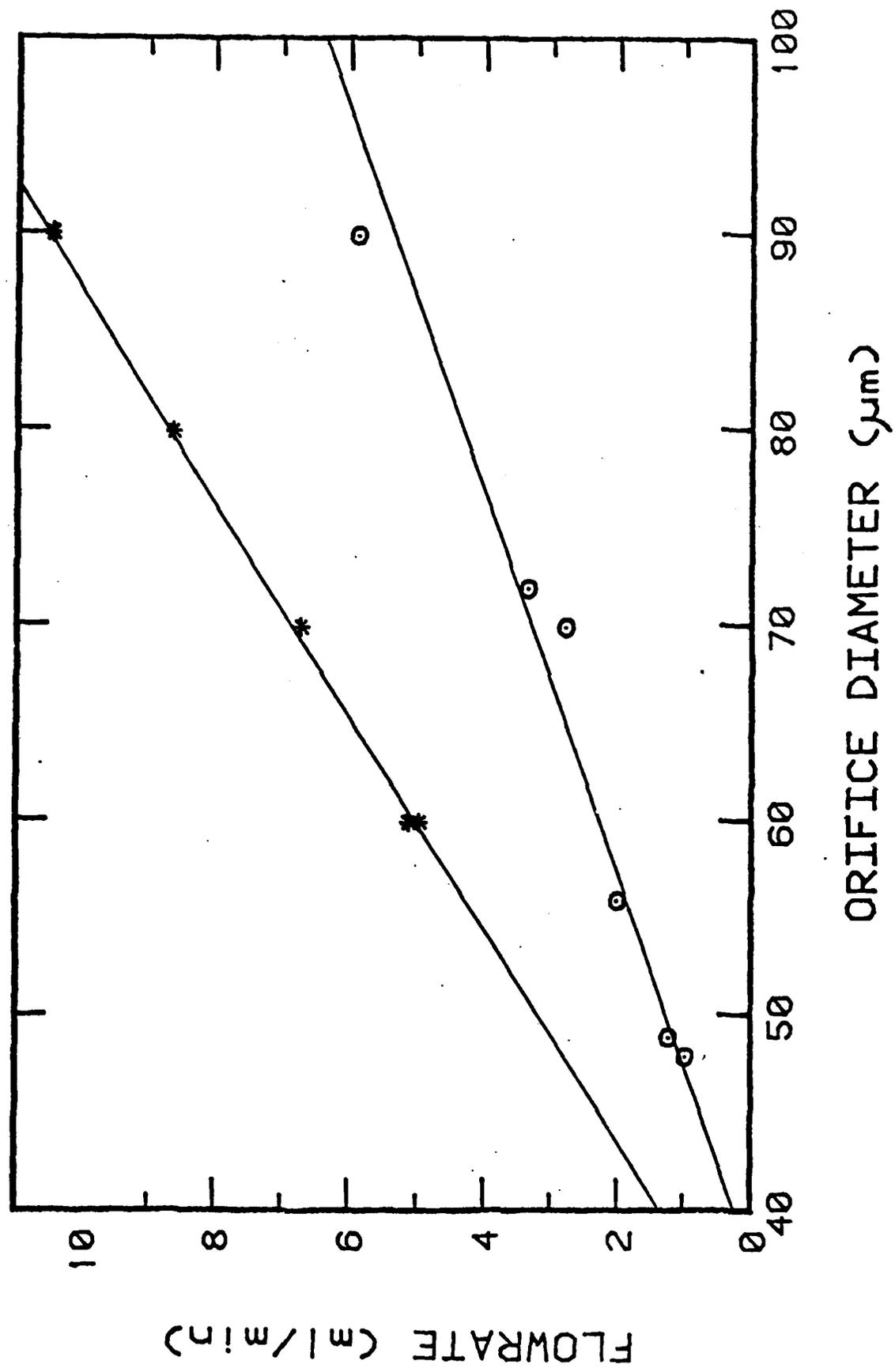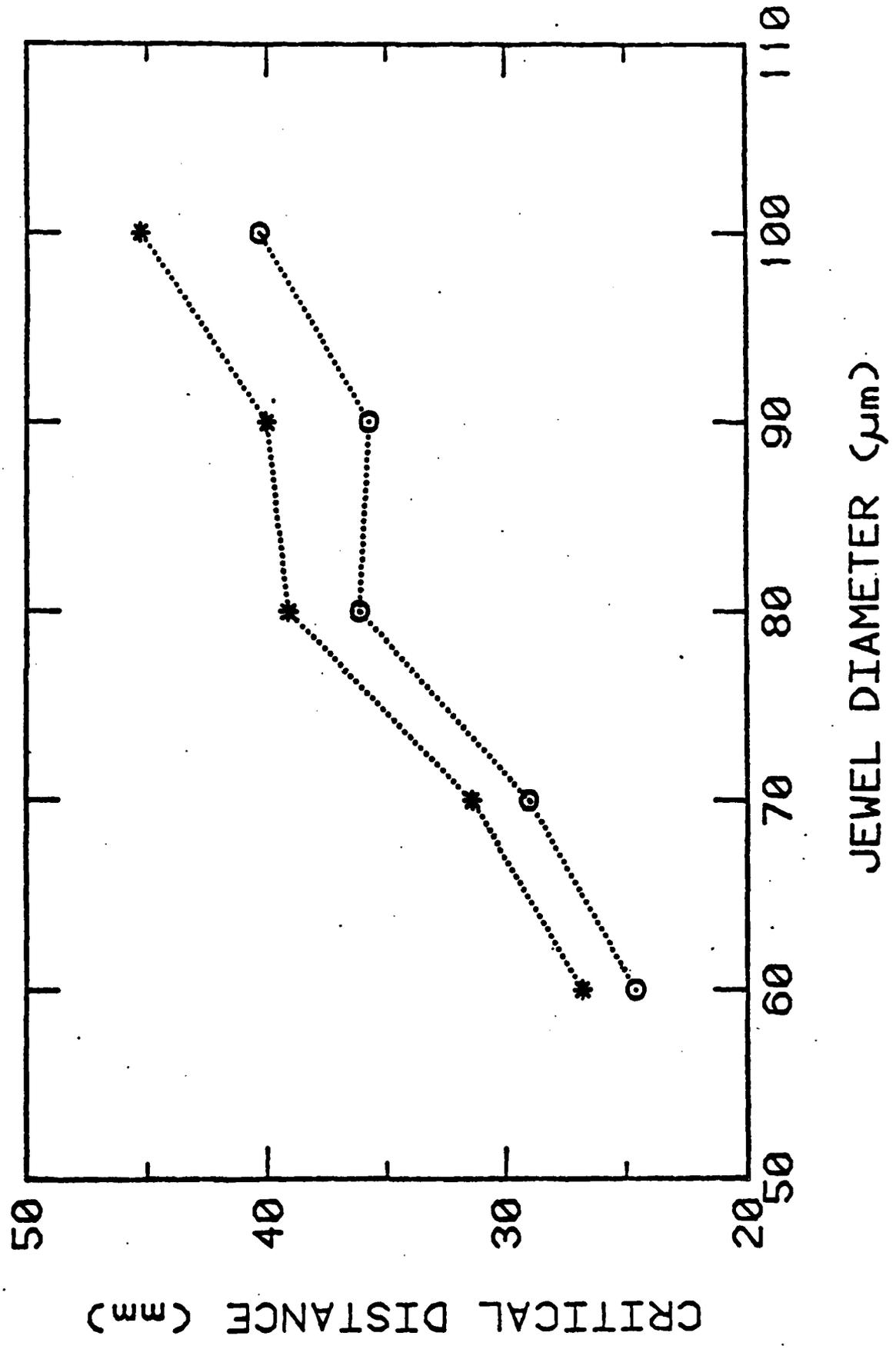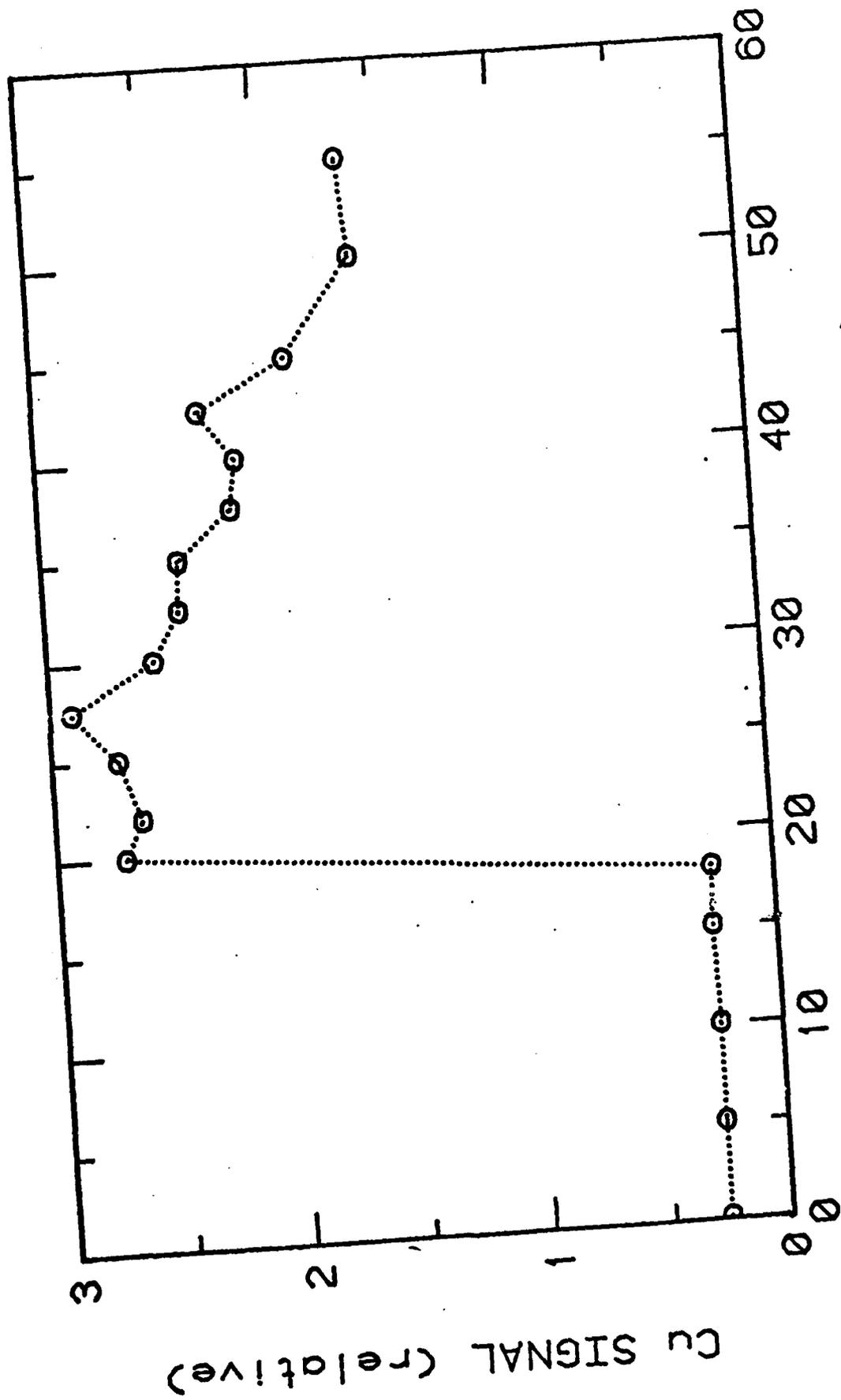
JET VELOCITY (m/sec)
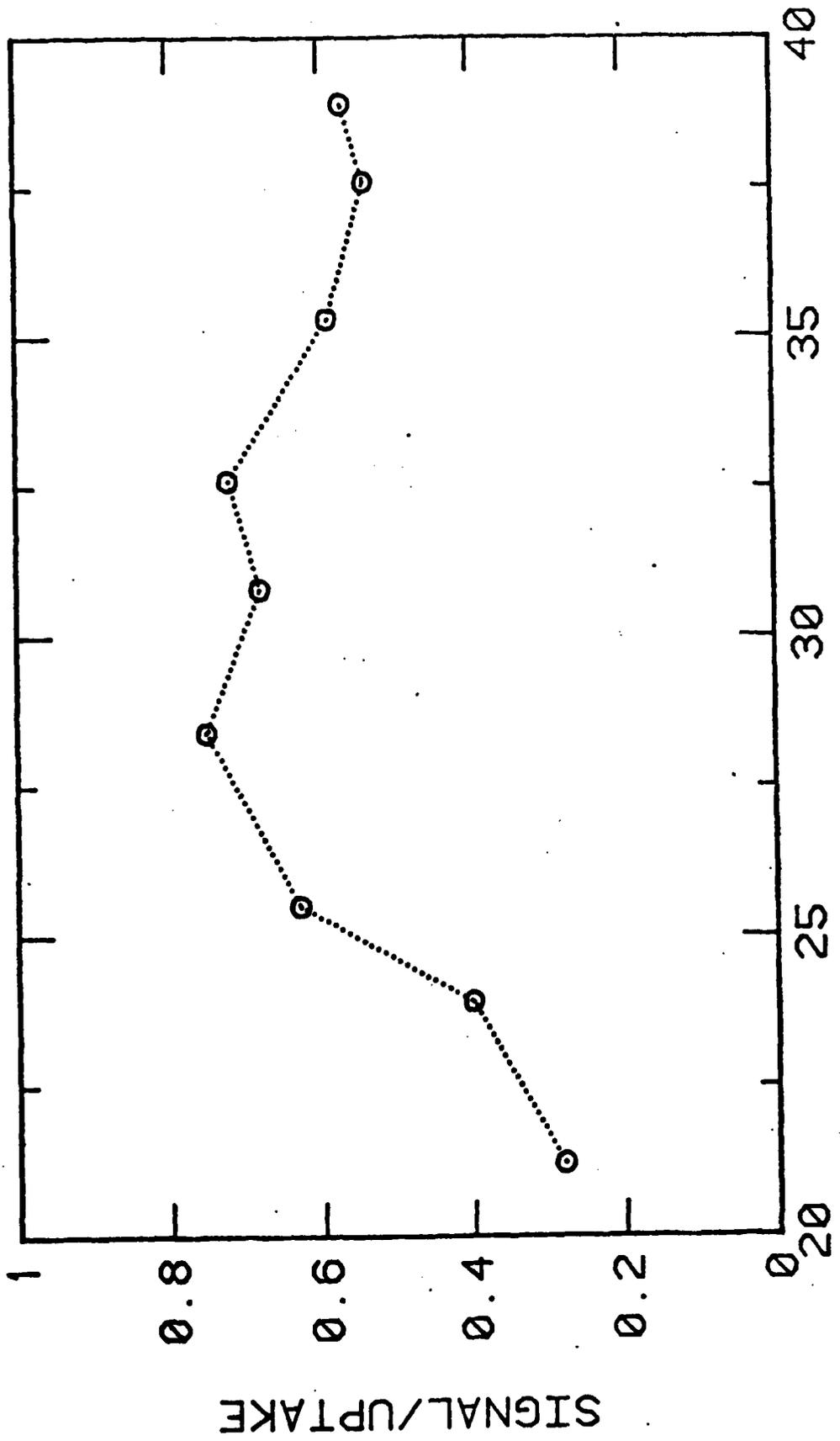
Fig 7

Fig. 9
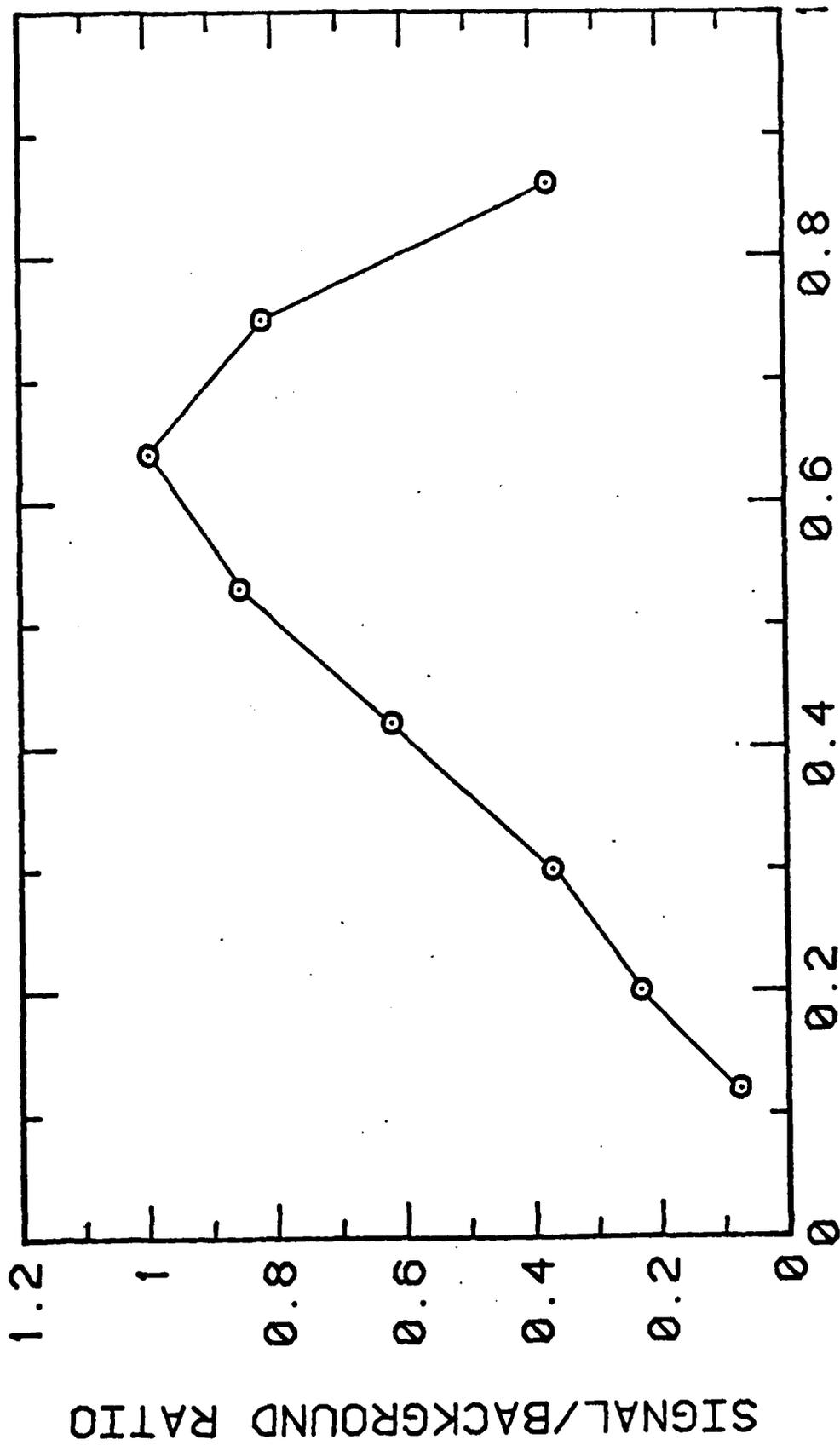
SIGNAL/BACKGROUND RATIO vs **CARRIER GAS FLOWRATE (L/min)**
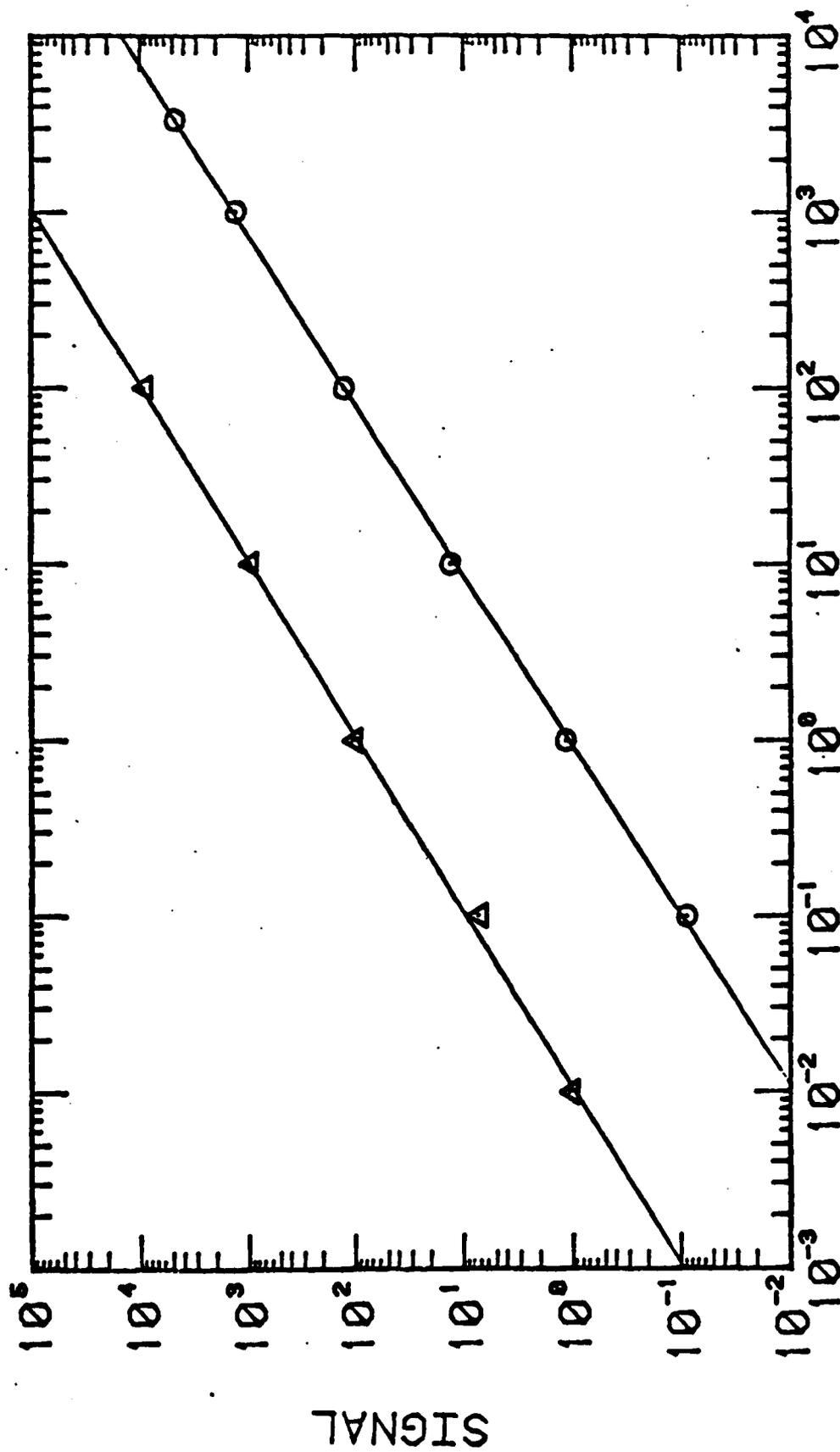
CONCENTRATION (ug/mL)

SIGNAL

Fig. 3

TECHNICAL REPORT DISTRIBUTION LIST, 051C

	No. Copies		No. Copies
Dr. M. B. Denton Department of Chemistry University of Arizona Tucson, Arizona 85721	1	Dr. L. Jarris Code 6100 Naval Research Laboratory Washington, D.C. 20375	1
Dr. R. A. Osteryoung Department of Chemistry State University of New York at Buffalo Buffalo, New York 14214	1	Dr. John Duffin, Code 62 Dn United States Naval Postgraduate School Monterey, California 93940	1
Dr. J. Osteryoung Department of Chemistry State University of New York Buffalo, New York 14214	1	Dr. G. M. Hieftje Department of Chemistry Indiana University Bloomington, Indiana 47401	1
Dr. B. R. Kowalski Department of Chemistry University of Washington Seattle, Washington 98105	1	Dr. Victor L. Rehn Naval Weapons Center Code 3813 China Lake, California 93555	1
Dr. S. P. Perone Department of Chemistry Purdue University Lafayette, Indiana 47907	1	Dr. Christie G. Enke Michigan State University Department of Chemistry East Lansing, Michigan 48824	1
Dr. D. L. Venezky Naval Research Laboratory Code 6130 Washington, D.C. 20375	1	Dr. Kent Eisentraut, MBT Air Force Materials Laboratory Wright-Patterson AFB, Ohio 45433	1
Dr. H. Freiser Department of Chemistry University of Arizona Tucson, Arizona 85721		Walter G. Cox, Code 3632 Naval Underwater Systems Center Building 148 Newport, Rhode Island 02840	1
Dr. H. Chernoff Department of Mathematics Massachusetts Institute of Technology Cambridge, Massachusetts 02139	1	Professor Isiah M. Warner Department of Chemistry Emory University Atlanta, Georgia 30322	
Dr. A. Zirino Naval Undersea Center San Diego, California 92132	1	Professor George H. Morrison Department of Chemistry Cornell University Ithaca, New York 14853	1

TECHNICAL REPORT DISTRIBUTION LIST, 051C

No.
Copies

No.
Copie

Professor J. Janata
Department of Bioengineering
University of Utah
Salt Lake City, Utah 84112   1

Dr. Carl Heller
Naval Weapons Center
China Lake, California 93555   1

Dr. Denton Elliott
AFOSR/NC
Bolling AFB
Washington, D.C. 20362

Dr. J. Decorpo
NAVSEA-05R14
Washington, D.C. 20362

Dr. B. E. Spielvogel
Inorganic and Analytical Branch
P. O. Box 12211
Research Triangle Park, NC 27709

Dr. Charles Anderson
Analytical Chemistry Division
Athens Environmental Lab.
College Station Road
Athens, Georgia 30613

Dr. Samual P. Perone
L-326
LLNL
Box 808
Livermore, California 94550

Dr. B. E. Douda
Chemical Sciences Branch
Code 4052
Naval Weapons Support Center
Crane, Indiana 47522

Ms. Ann De Witt
Material Science Department
160 Fieldcrest Avenue
Raritan Center
Edison, New Jersey 08818

TECHNICAL REPORT DISTRIBUTION LIST, GEN

	No. Copies		No. Copies
Office of Naval Research Attn: Code 413 800 North Quincy Street Arlington, Virginia 22217	2	Naval Ocean Systems Center Attn: Mr. Joe McCartney San Diego, California 92152	1
ONR Pasadena Detachment Attn: Dr. R. J. Marcus 1030 East Green Street Pasadena, California 91106	1	Naval Weapons Center Attn: Dr. A. B. Amster, Chemistry Division China Lake, California 93555	1
Commander, Naval Air Systems Command Attn: Code 310C (H. Rosenwasser) Department of the Navy Washington, D.C. 20360	1	Naval Civil Engineering Laboratory Attn: Dr. R. W. Drisko Port Hueneme, California 93401	1
Defense Technical Information Center Building 5, Cameron Station Alexandria, Virginia 22314	12	Dean William Tolles Naval Postgraduate School Monterey, California 93940	1
Dr. Fred Saalfeld Chemistry Division, Code 6100 Naval Research Laboratory Washington, D.C. 20375	1	Scientific Advisor Commandant of the Marine Corps (Code RD-1) Washington, D.C. 20380	1

U.S. Army Research Office
Attn: CRD-AA-IP
P. O. Box 12211
Research Triangle Park, N.C. 27709
	1	Naval Ship Research and Development
		    Center
		Attn: Dr. G. Bosmajian, Applied
		    Chemistry Division
		Annapolis, Maryland 21401
			1

Mr. Vincent Schaper DTNSRDC Code 2803 Annapolis, Maryland 21402	1	Mr. John Boyle Materials Branch Naval Ship Engineering Center Philadelphia, Pennsylvania 19112	1
Naval Ocean Systems Center Attn: Dr. S. Yamamoto Marine Sciences Division San Diego, California 91232	1	Mr. A. M. Anzalone Administrative Librarian PLASTEC/ARRADCOM Bldg 3401 Dover, New Jersey 07801	1

END

FILMED

10-83

DTIC